

# Open-World Entity Segmentation

Lu Qi<sup>1†</sup>, Jason Kuen<sup>2†</sup>, Yi Wang<sup>1</sup>, Jiuxiang Gu<sup>2</sup>, Hengshuang Zhao<sup>3</sup>, Zhe Lin<sup>2</sup>, Philip Torr<sup>3</sup>, Jiaya Jia<sup>1</sup>

<sup>1</sup>The Chinese University of Hong Kong <sup>2</sup>Adobe Research <sup>3</sup>University of Oxford

## Abstract

We introduce a new image segmentation task, called *Entity Segmentation (ES)*, which aims to segment all visual entities (objects and stuffs) in an image without predicting their semantic labels. By removing the need of class label prediction, the models trained for such task can focus more on improving segmentation quality. It has many practical applications such as image manipulation and editing where the quality of segmentation masks is crucial but class labels are less important. We conduct the first-ever study to investigate the feasibility of convolutional center-based representation to segment things and stuffs in a unified manner, and show that such representation fits exceptionally well in the context of ES. More specifically, we propose a CondInst-like fully-convolutional architecture with two novel modules specifically designed to exploit the class-agnostic and non-overlapping requirements of ES. Experiments show that the models designed and trained for ES significantly outperforms popular class-specific panoptic segmentation models in terms of segmentation quality. Moreover, an ES model can be easily trained on a combination of multiple datasets without the need to resolve label conflicts in dataset merging, and the model trained for ES on one or more datasets can generalize very well to other test datasets of unseen domains. The code has been released at <https://github.com/dvlab-research/Entity>.

## 1. Introduction

In recent years, image segmentation tasks (semantic segmentation [8, 9, 26, 43, 49, 87, 88], instance segmentation [13, 21, 38, 46, 57, 70, 75, 76, 78], and panoptic segmentation [7, 33, 34, 39, 81], etc.) have received great attention due to their diverse applications [6, 51, 54, 61, 62, 64] and strong progress made possible by deep learning [22, 23, 25, 35, 65, 67, 68]. Most image segmentation tasks share the common goal of automatically assigning each image pixel to one of the predefined semantic classes. One of the key application areas of image segmentation is image manipulation [27, 66,

73, 77, 85, 86] and editing [2, 16, 36, 52]. Segmentation techniques have revolutionized image manipulation and editing applications by enabling users to operate directly on semantically-meaningful regions, as opposed to primitive image elements such as pixels and superpixels.

Although image segmentation holds much promise for user-friendly image manipulation and editing, there are two major weaknesses in image segmentation that adversely affect the image manipulation/editing experience: 1) class label confusion (often caused by having many predefined class labels); 2) lack of generalization for unseen classes. In Fig. 1, we present the segmentation results from a state-of-the-art panoptic segmentation method [39] that demonstrate the two weaknesses separately. These weaknesses can be largely attributed to the standard practice of training models to segment strictly based on the predefined classes.

In image manipulation and editing applications, where class labels are typically not required, the conventional class-specific image segmentation may be sub-optimal and could introduce unnecessary class-related issues. Is there a better alternative to class-specific image segmentation? Yes, it comes from omitting the classification subtask and focusing solely on the segmentation subtask, in a similar spirit to the class-agnostic RPN [60]. This is analogous to infants capable of distinguishing objects by shapes and appearances without knowing the object names [17]. Without the need to assign class labels, the class confusion issue can be largely alleviated. Besides, as demonstrated in object detection [28, 59], class agnosticism provides a strong generalization to unseen classes. Furthermore, it is likely to relieve the model’s burden of trading off segmentation mask quality against classification performance.

To this end, we propose a new image segmentation task named *Entity Segmentation (ES)* which aims to generate class-agnostic segmentation masks of an image. We leverage the existing panoptic segmentation datasets [12, 42, 90] with both instance (*thing*) and non-instance (*stuff*) masks, but universally treat any of the annotated *thing* and *stuff* masks as a class-agnostic *entity*. Since the popular class-specific Panoptic Quality (PQ) metric [34] is not

<sup>†</sup>Equal contribution.

<sup>1</sup>PanopticFCN [39] with ResNet101 [22] backbone and Deformable Convolution v2 [15, 91].

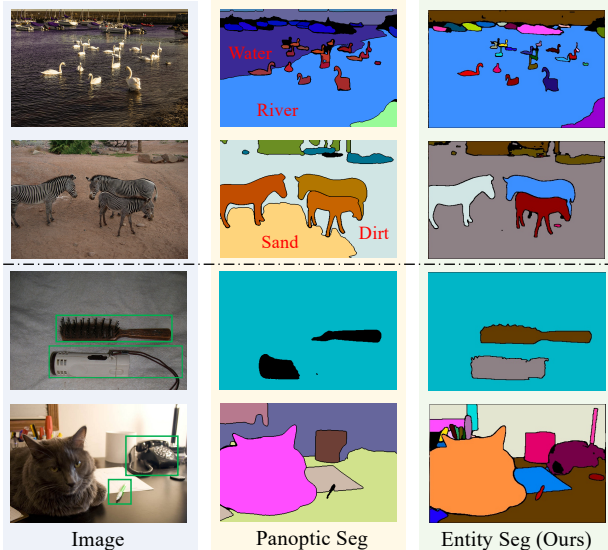


Figure 1. The first two columns show the examples of class confusion. Even with a state-of-the-art panoptic segmentation network<sup>1</sup>, there tends to be two or more masks with semantically-overlapped classes (e.g., *river* & *water*, *sand* & *dirt*) predicted for a single entity. The last two second columns illustrate that the network has troubles segmenting unseen objects like *afro pick*, *pencil*, *telephone*.

directly applicable to our task, we introduce a class-agnostic metric  $AP_e$  with a strict non-overlapping mask constraint. This constraint aligns well with image editing/manipulation applications that expect each image pixel to only correspond to a single entity.

Given our proposed new task and evaluation metric, we aim to devise a conceptually simple and effective framework to tackle the task. The center-based output representation (i.e., representing objects by their centers) has enabled recent one-stage object detectors [41, 71] to achieve strong performance and fast training. Inspired by that, we carry out the first-ever study to investigate the feasibility of using such a representation uniformly for all entities including *stuffs*. Our study reveals a strong and previously-unknown evidence that a fully-convolutional network paired with the center-based representation can effectively handle the task. We are the first to challenge the common understanding that the difficult-to-train Transformer decoder [7, 11] is necessary to unify the representation for *things* and *stuffs*.

Based on our findings, we introduce a fully-convolutional segmentation framework inspired by CondInst [70] to detect and segment all entities (regardless of *thing* or *stuff*) in a unified manner. To better exploit the unique *class-agnostic* and *non-overlapping* requirements of ES, we propose a global kernel bank module and an overlap suppression module that substantially improve the

framework and thus boost the performance on the ES task. The global kernel bank module generates mask kernels to exploit some common properties (e.g, textures, edges) shared by many entities, while the overlap suppression module encourages the predicted masks not to overlap with each other.

Extensive experiments on the challenging COCO dataset [42] show the effectiveness of our proposed method. Furthermore, we study the generalization ability of our COCO-trained model through a cross-dataset evaluation on ADE20K [90]. Our model shows superior performance both quantitatively and qualitatively on such a dataset despite that it has not been trained on it. As shown in Fig. 4, the model is able to correctly segment the entities belonging to unseen classes. These suggest that the models trained for the proposed ES task are naturally capable of open-world image segmentation.

Overall, our contributions are summarized as follows:

- We propose a task called Entity Segmentation which aims to segment every visual entity without predicting its class label or identifying it as *thing* or *stuff*.
- We conduct the first-ever study to investigate the feasibility of convolutional center-based representation for various tasks and surprisingly find that all entities (regardless of *thing* or *stuff*) can be effectively represented by such a representation in a unified manner.
- Our findings lead us to devise a fully-convolutional segmentation framework inspired by CondInst. We introduce two novel modules to our framework to better exploit the unique requirements of the ES task.
- We conduct extensive experiments and demonstrate the remarkable effectiveness and generalization of our proposed task and segmentation framework.

## 2. Related Work

**Image segmentation.** Image segmentation is the process of partitioning a digital image into multiple segments (sets of pixels, also known as image objects) [69]. The main tasks of image segmentation include salient object detection [4, 5, 31, 37, 58], semantic segmentation [8–10, 26, 43, 49, 80, 82–84, 87, 88], instance segmentation [13, 21, 38, 46, 57, 70, 75, 76, 78], and panoptic segmentation [7, 33, 34, 39, 44, 81]. Salient object detection mimics the behavior of human in focusing on the most salient region/object in an image while ignoring the class it belongs to [72]. In contrast, semantic/instance/panoptic segmentation aims at densely assigning each image pixel to the one of classes predefined in the training datasets. The segmentation models trained for these tasks are required to make a trade-off between

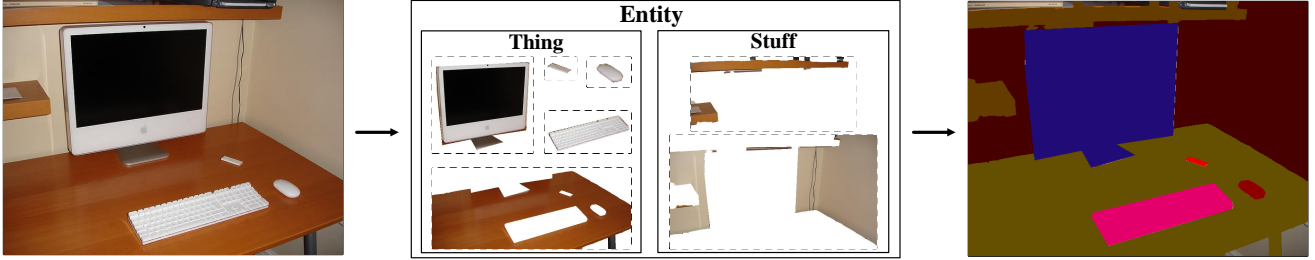


Figure 2. The ground-truth annotations of entity segmentation. To convert the annotations of panoptic segmentation to entity segmentation format, we regard each *thing* or *stuff* as an independent entity, even though some of them may have multiple disconnected parts.

the mask prediction and classification subtasks in terms of performance. Moreover, such tasks tightly couple segmentation and classification. As a result, it is not easy to independently evaluate the segmentation and classification strengths of their segmentation models.

In this work, we provide a new perspective on image segmentation by introducing the entity segmentation task that handles dense image segmentation similarly as semantic/instance/panoptic segmentation, but without the classification aspect akin to salient object detection. This task focuses only on class-agnostic segmentation. It treats every segment (whether *thing* or *stuff*) as a visual entity. Compared to the existing segmentation tasks, it is more useful for user-friendly image manipulation and editing applications in which the segmentation mask quality is of utmost importance.

**Object detection.** Object detection [14, 19, 20, 40, 41, 55, 60, 71] requires detecting objects with bounding box representation. The methods can be partitioned into two types: (1) one-stage [41, 71] detectors that detect objects using pixelwise features at dense pixel locations; (2) two-stage detectors [19, 20, 40, 60] that first predict class-agnostic region proposals and subsequently perform classification based on region-of-interest (RoI) features and a separate classification head.

In this paper, our method is built upon FCOS [71], a standard one-stage detector, to detect entities. Different from the standard definition of *object*, entity is a more general concept that includes both objects/*things* and *stuffs*. To our best knowledge, our method is the first to demonstrate that center-based detection can effectively handle all entities in a uniform manner, contrary to the existing practice of separately. In contrast to DETR [7] and MaskFormer [79], our segmentation framework neither requires an excessively long training duration (12 vs 300 epochs) nor strong data augmentation.

**Open-world detection & segmentation.** The open-world setting has been explored in the contexts of object detection

and segmentation [3, 18, 24, 29, 32, 48, 53, 74] with the general goal of identifying new object classes given a closed-world training dataset. Generally, previous open-world methods explicitly differentiate *unknown* and *known* objects by spotting outliers in the embedding space. On the contrary, our entity segmentation task is class-agnostic and does not need to distinguish between *unknown* and *known* classes, allowing the segmentation models to focus entirely on the segmentation task itself.

### 3. Entity Segmentation

**Task definition.** The task of entity segmentation (ES) is defined as segmenting all visual entities within an image in a class-agnostic manner. Here, “entity” refers to either a *thing* (instance) mask or a *stuff* mask in the common context. This definition is related to the standard and well-accepted definition of “object” which is based on certain objectness properties introduced by the seminal work [1]: (a) a well-defined closed boundary in space; (b) a different appearance from their surroundings. As illustrated in Fig. 2, an entity can be any semantically meaningful and coherent region in the open-world setting, e.g., person, television, wall. Given the subjective nature of this task, we conduct a comprehensive user study to validate the personal intuitions for the concept of entity, as reported in the *supplementary*.

**Task format.** Given an input image  $\mathbf{I} \in \mathbb{R}^{H \times W \times 3}$ , the task expects a pixel-wise prediction map  $\mathbf{P} \in \{1, \dots, N\}^{H \times W}$  and a list of confidence scores  $\mathbf{S} \in \mathbb{R}^N$  as the output that contains the non-overlapping IDs of the predicted  $N$  entities and their confidence scores. Ground truth annotations are encoded in an identical manner as the prediction map. There are no semantic class labels involved and all entities are treated equally without the distinction of *thing* and *stuff*.

**Relationship to similar tasks.** The newly proposed task is focused on the concept of “entity”. It is related to but different from several previous tasks. Different from *semantic segmentation*, ES is instance-aware. In contrast to *instance segmentation*, ES includes *stuff* masks in

Subset	Class-agnostic		AP <sup>b</sup>	AP <sup>b</sup> <sub>50</sub>	AP <sup>b</sup> <sub>75</sub>	AP <sup>b</sup> <sub>S</sub>	AP <sup>b</sup> <sub>M</sub>	AP <sup>b</sup> <sub>L</sub>	
	training	evaluation							
Thing	○	○	37.4	56.0	39.9	15.5	36.5	50.5	← ref
	○	✓	40.9	63.9	43.4	18.6	42.1	60.7	
	✓	✓	41.6	64.6	43.9	18.5	42.7	61.7	
Stuff	○	○	23.2	35.4	23.5	1.4	5.9	26.9	
	○	✓	38.7	58.4	39.3	1.8	7.2	46.6	
	✓	✓	39.4	60.5	39.3	1.4	6.4	47.2	
Thing & Stuff (Entity)	○	○	29.5	45.2	31.0	9.2	23.6	38.0	
	○	✓	37.6	60.2	39.3	16.5	35.0	49.5	
	✓	✓	39.2	62.5	40.4	16.6	35.5	51.1	

Table 1. Study on the feasibility of convolutional center-based representation [71, 75] on different class-agnostic/specific detection tasks that involve *thing* and *stuff*. *Subset* refers to the subset of COCO training/validation set with the annotations from one of: *thing*, *stuff*, or *thing&stuff* (Entity). ○/✓ signifies that we do/do-not use class information in the training or evaluation stage. AP<sup>b</sup> is the box-based AP.

addition to instance masks. Moreover, unlike the above-mentioned segmentation tasks and the more recent *panoptic segmentation*, ES completely omits the class labels and classification functionality.

**Annotation transformation.** Given the commonalities with panoptic segmentation, the annotations in existing panoptic segmentation datasets can be directly transformed into the format defined for ES. As shown in Fig. 2, each *thing* or *stuff* mask is simply regarded as an independent entity.

**Evaluation metric.** Due to the non-overlapping requirement in downstream image manipulation and editing applications, we propose a new mask-based mean average precision for measurement, denoted as AP<sup>m</sup><sub>c</sub>. AP<sup>m</sup><sub>c</sub> follows closely the AP<sup>m</sup> used in instance segmentation [13, 21, 38, 46, 57, 70, 75, 76, 78], except that the AP<sup>m</sup><sub>c</sub> gives zero tolerance to mask overlaps of different entities. This simple constraint leads to a lower evaluation number than instance segmentation’s AP<sup>m</sup>, since it makes the metric significantly more sensitive to the class-agnostic duplicate removal [56] performance and mask quality. In our experiment, the number drops by 4.7 if AP<sup>m</sup><sub>c</sub> is used in place of AP<sup>m</sup>.

#### 4. Unified Entity Representation

The output representation is a defining aspect of any segmentation tasks. Given the close relationship of ES with panoptic segmentation, we first discuss panoptic representation. Due to the different natures of *thing* (instance) and *stuff* (non-instance) classes, existing panoptic segmentation methods usually adopt separate strategies [33, 81] for the two outputs. In particular, they are handled through a divide-and-conquer pipeline, *i.e.*, using a branch that emphasizes explicit localization cues for things, while using another branch that focuses on semantic consistency for *stuff* [39]. However, due to the lack of both class labels and *thing-stuff* separation in our ES task, the existing panoptic representation is incompatible with ES and thus existing panoptic approaches are not directly applicable to ES.

As with panoptic segmentation, the question of “how

to represent entities?” is crucial to ES. The center-based representation used by convolutional networks to represent objects by their center locations is a promising form of representation already been proven effective and efficient for object/*thing*-level tasks (*e.g.*, object detection [41, 71] and instance segmentation [57, 70, 78]), but its feasibility on *stuffs* (and entities) has not been investigated and remains unknown. To answer the aforementioned question, we present the first-ever study<sup>1</sup> to investigate the feasibility of using center-based representation to represent *stuffs* and entities. The study is carried out through the proxy tasks of class-specific and -agnostic box-level detection. Class-agnostic detection can be seen as the box-level counterpart of ES, and thus the conclusion derived from this study should be largely applicable to ES.

The results of the study are provided in Table 1. The first row indicated by *ref* is the reference model based on the conventional object detection task that the center-based representation is originally designed for. Thus, the representation is deemed effective for a particular task (a row in the table) if it achieves APs that are comparable or higher than those of *ref*. It can be clearly seen that the representation is effective for most of the tasks, except for the class-specific *stuff*-only and *thing-stuff* tasks which have much weaker performances. This finding suggests that the center-based representation is poorly effective only if both of these conditions are satisfied: (1) task is class-specific; (2) *stuffs* are involved. Furthermore, we find that the representation has a surprisingly strong compatibility with all the tasks with class-agnostic training, as demonstrated by their excellent APs. These two interesting findings provide us with a powerful support as to why using the center-based representation to handle both *things* and *stuffs* in a unified manner is the right choice for ES, but it is not necessarily the case for existing class-specific tasks that involve *stuffs*, such as panoptic segmentation.

<sup>1</sup>For the models evaluated in the study, we adopt FCOS [71] with ResNet50 backbone and default training hyperparameters.



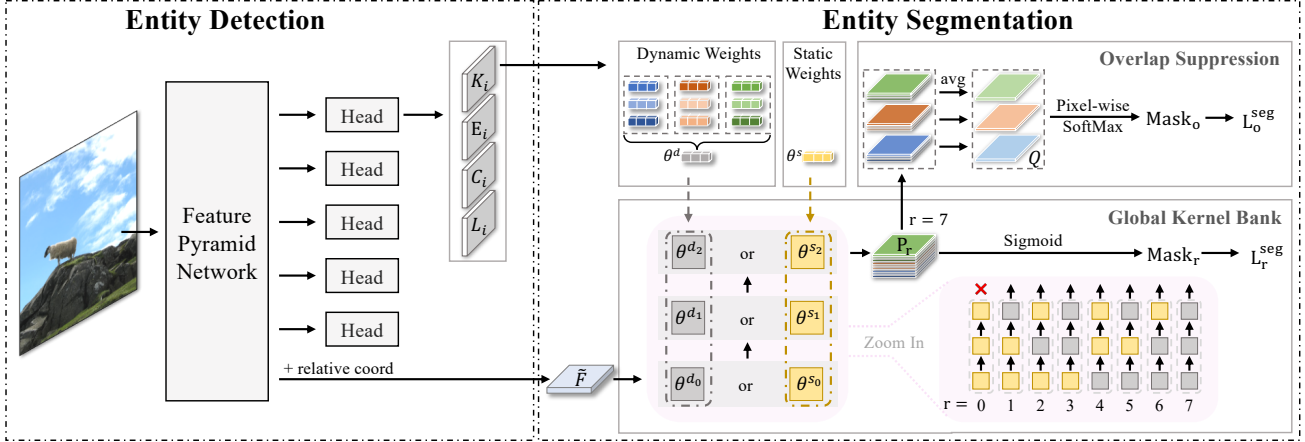


Figure 3. The entity segmentation framework. For the part of entity detection, we directly follow the design of FCOS detector [71]. The entity masks are generated by convolving the low-level feature map  $\tilde{F}$  with dynamic weights  $\theta^d$ . In our method, we propose the global kernel bank and overlap suppression modules to exploit class-agnostic and non-overlapping requirements of  $\theta^d$ . The  $L_o^{seg}$  here stands for  $L_{o,r=7}^{seg}$  which indicates that the global kernel bank’s path ( $r=7$ ) with all dynamic weights is used for the overlap suppression module.

## 5. Method

As mentioned in Sec. 4, all entities are represented by the center-based unified entity representation – i.e., we represent each entity (including *stuffs*) by the *mass center* of its mask, similar to how objects are represented by their bounding-box centers [71]. In this section, we first describe how we devise an *Entity segmentation framework* based on the unified center-based representation. Then, we introduce two novel modules: *global kernel bank* and *overlap suppression*, to exploit the requirements of ES in order to improve the segmentation quality of predicted entity masks.

### 5.1. Segmentation Framework

As described in Sec. 3, a non-overlapping entity ID prediction map  $\mathbf{P}$  and a list of confidence score map  $\mathbf{S}$  are expected, given an input  $\mathbf{I}$ . Inspired by recent one-stage segmentation approaches [39, 57, 70, 76], we adopt a similar *generate-kernel-then-segment* pipeline. Specifically, with a single stage feature  $\mathbf{X}_i \in \mathbb{R}^{H_i \times W_i \times C_i}$  from the  $i$ -th stage in Feature Pyramid Network (FPN) [40], four branches are added to handle the four output types required to perform ES: *entityness*, *centerness*, *localization*, and *kernel*. Here, entityness and centerness branches respectively provide a probability map  $\mathbf{E}_i \in [0, 1]^{H_i \times W_i}$  and a centerness map  $\mathbf{C}_i \in [0, 1]^{H_i \times W_i}$ .  $\mathbf{E}_i$  indicates each pixel’s probability of being an entity, while  $\mathbf{C}_i$  estimates centerness values [71]. Localization branch is used to regress the bounding box offsets  $\mathbf{L}_i$  of entities, which are used for efficient non-maximum suppression (NMS). For mask generation, we draw inspirations from dynamic kernel work [30, 39, 57, 70] and employ a kernel branch to generate entity-specific dynamic kernel weights.

### 5.2. Global Kernel Bank

The use of dynamic kernels to generate entity masks assumes that the cues needed to segment different entities are dissimilar, but there exists many common properties (e.g. textures, edges) which are shared by different entities. This motivates us to leverage static kernel weights for training the mask head, alongside the dynamic kernel weights. The combination of dynamic and static kernel weights, referred to as *global kernel bank*, allows the network to strike a good balance between learning entity-specific features and becoming aware of features that are commonly useful to many entities.

Global kernel bank consisting of three pairs of dynamic and static convolutions can be easily incorporated into our segmentation framework. To strengthen the interactions between dynamic and static kernels, we allow either dynamic or static kernels at each convolutional layer, resulting in seven possible network paths (minus the one with solely static kernels) in a 3-layer mask head, as presented in Fig. 3. During training, we train with all seven paths simultaneously to minimize the mask prediction (Dice [50]) loss with respect to ground truth  $\mathbf{Y}$ :

$$\mathcal{L}_r^{seg} = \lambda_r \times \text{Dice}(\text{Sigmoid}(\text{MaskHead}(\tilde{\mathbf{F}}; \theta_r)), \mathbf{Y}), \quad (1)$$

where  $r$  and  $\lambda_r$  respectively denote the path’s index and the path-specific hyperparameter that weights the loss.  $\tilde{\mathbf{F}} \in \mathbb{R}^{H/8 \times W/8 \times (C_{mask}+2)}$  indicates the concatenation of backbone features (encoded for mask prediction) and relative coordinates [45]. The kernels denoted by  $\theta_r$  can be represented more granularly by  $\theta_r^{vu}$  to indicate its kernel type ( $v \in \{s: \text{static}, d: \text{dynamic}\}$ ) and convolutional layer index ( $u \in \{0, 1, 2\}$ ) in MaskHead. Given  $\theta_r^{vu}$ , the MaskHead for each path  $r$  is defined as follows

$$\begin{aligned}
\text{MaskHead}(\tilde{\mathbf{F}}; \theta_1) &= \otimes (\theta_1^{s_0}, \otimes(\theta_1^{s_1}, \otimes(\theta_1^{d_2}, \tilde{\mathbf{F}}))) \\
\text{MaskHead}(\tilde{\mathbf{F}}; \theta_2) &= \otimes (\theta_2^{s_0}, \otimes(\theta_2^{d_1}, \otimes(\theta_2^{s_2}, \tilde{\mathbf{F}}))) \\
&\vdots \\
\text{MaskHead}(\tilde{\mathbf{F}}; \theta_7) &= \otimes (\theta_7^{d_0}, \otimes(\theta_7^{d_1}, \otimes(\theta_7^{d_2}, \tilde{\mathbf{F}}))),
\end{aligned} \tag{2}$$

where  $\otimes(\cdot, \cdot)$  indicates the spatial convolution operation.

Despite the many paths trained, during inference, we find that using the path with solely dynamic kernels  $\theta_7$  alone is sufficiently effective while being computationally efficient.

### 5.3. Overlap Suppression

The ES task (Sec. 2) expects no overlapping masks. However, dynamic kernel-based approaches tend to generate overlapping masks with high confidence due to the concept overlap among adjacent entities and independent losses being used for different kernels. Although postprocessing strategies [33, 39] can resolve mask overlaps, they are driven by handcrafted heuristics which are less effective. Instead, we propose a module that encourages the model to learn to suppress the overlaps among the predicted entity masks.

During training, there are  $M$  number of sampled kernels and each of the  $M$  kernels is assigned to one of the  $N$  ground-truth entities according to the mask-based sample assignment strategy [70]. This can be viewed as having  $N$  clusters with one or more kernels within each cluster. Considering that the 7<sup>th</sup> path (all dynamics weights) is the only path used for inference, we only perform overlap suppression for this path. First, we obtain the *representative* mask  $\mathbf{Q}^n$  of the  $n$ -th cluster by averaging all its masks generated via  $\theta_7$ :

$$\mathbf{Q}^n = \frac{\sum_{i \in \Omega(n)} \text{MaskHead}(\tilde{\mathbf{F}}; \theta_{7|i})}{|\Omega(n)|} \tag{3}$$

where  $\Omega(n)$  returns the set of kernel indices belonging to the  $n$ -th cluster and  $\theta_{7|i}$  indicates the  $i$ -th kernel in  $\theta_7$ . Given the representative entity masks  $\mathbf{Q}$ , we apply pixelwise softmax function to induce a strong suppression of non-maximal entities in the pixel-wise mask prediction. To achieve overlap suppression, we adopt a separate training loss similar to  $\mathcal{L}_r^{seg}$  (Eq. 1):

$$\mathcal{L}_o^{seg} = \text{Dice}(\text{Softmax}(\mathbf{Q}), \mathbf{Y}), \tag{4}$$

Note that the pixels without annotations are ignored in  $\mathcal{L}_o^{seg}$ .

### 5.4. Training and Inference

In the training stage, the segmentation network is trained with the overall loss defined as:

$$\mathcal{L} = \mathcal{L}^{det} + \mathcal{L}_o^{seg} + \mathcal{L}_R^{seg} = \mathcal{L}^{det} + \mathcal{L}_o^{seg} + \sum_r \mathcal{L}_r^{seg}. \tag{5}$$

In the inference stage, we first sort all entity detections according to their (aggregated) confidence scores:  $\sqrt{\mathbf{C}_i(\text{centerness}) \times \mathbf{E}_i(\text{entityness probability})}$ , and their corresponding boxes are obtained from the localization branch and then processed with box-level NMS. After the duplicate removal, each remaining entity is encoded into an entity-specific dynamic kernel, resulting in  $N$  kernels for  $N$  entities. With the generated dynamic kernels and encoded features shown in Fig. 3, the segmentation masks  $\hat{\mathbf{Y}} \in \mathbb{R}^{N \times H_3 \times W_3}$  of  $N$  entities are produced by a sequence of convolutions directly. Finally, the final non-overlapping prediction map  $\mathbf{P}$  is acquired by choosing the entity ID with the maximum confidence score at each pixel [33].

## 6. Experiments

### 6.1. Main Evaluation

We perform the main evaluation studies through the single-dataset setting on COCO dataset [42]. Following the common practice, we train our models with 118,287 train images and reported results on the 5,000 validation images. Unless specified, we train our network with ImageNet-pretrained ResNet-50 [22] backbone using batch size 16 for 12 epochs. The longer edge sizes of the images is 1333. The shorter edge sizes of the images is random sampled from 640 to 800 with stride 32. We decay the learning rate with 0.1 after 8 and 11 epochs respectively.

**Proposed two modules.** Table 2(a) summarizes the performance improvements introduced by the two proposed modules to the baseline. The baseline is a simple segmentation framework that uses only the loss  $\mathcal{L}_0^{seg}$  in mask branch, and it obtains 28.3 AP<sub>e</sub><sup>m</sup>. The incorporation of  $\mathcal{L}_R^{seg}$  and  $\mathcal{L}_o^{seg}$  improves it by 1.0, 0.8 AP<sub>e</sub><sup>m</sup>, respectively, demonstrating the effectiveness of the proposed modules. The last line shows that using these two modules achieves an even greater improvement of 1.5 AP<sub>e</sub><sup>m</sup>. This indicates that the two proposed modules are complementary with each other. Note that these two modules can bring consistent improvements even with a large state-of-the-art backbone. Particularly, with a large (L) Swin Transformer backbone, the two modules still provide a good performance gain of 1.4 AP<sub>e</sub><sup>m</sup>, as shown with more details in the *supplementary file*.

**Overlap suppression.** Table 2(b) provides the ablation study on the activation function used in  $\mathcal{L}_o^{seg}$ . Compared to the baseline without any activation function, Sigmoid and Softmax respectively bring 0.3 and 0.8 AP<sub>e</sub><sup>m</sup> improvements. Compared to Sigmoid, Softmax forces the network to suppress the mask prediction of non-maximal entities at every pixel and this helps to suppress mask overlaps more effectively. In the last row of Table 2(c), we use two  $\mathcal{L}_o^{seg}$  losses based on Sigmoid and Softmax separately, with a loss weight of 0.5 for each.

$\mathcal{L}_R^{seg}$ $\mathcal{L}_o^{seg}$   $AP_e^m$	Softmax   Sigmoid   $AP_e^m$	1   2   3   4   5   6   7   $AP_e^m$	Backbone   Epochs   $AP_e^m$
○ ○   28.3	○   ○   28.3	○ ○ ○ ○ ○ ○ ○   28.3	R-50   12   29.8
✓ ○   29.3	○   ✓   28.6	○ ○ ○ ○ ○ ○ ○   28.9	R-50   36   31.8
○ ✓   29.1	✓   ○   <b>29.1</b>	○ ○ ○ ○ ○ ✓ ✓ ✓   29.1	R-101   36   33.2
✓ ✓   <b>29.8</b>	✓   ✓   29.0	✓ ✓ ✓ ✓ ✓ ✓ ✓   <b>29.3</b>	R-101-DCNv2   36   <b>35.5</b>
(a)	(b)	(c)	(d)

Table 2. Ablation studies. ○ and ✓ respectively indicate whether a particular component is ablated or in used. **(a): Proposed two modules.** The impacts of global kernel bank and overlap suppression modules. **(b): Overlap suppression.** An ablation study of the scoring activation function in the module. **(c): The module of global kernel bank.** Each of “1,2,...,7” corresponds to the  $r$ -th path in global kernel bank, as in Fig. 3. **(d): High-Performance Regime.** The performance of our models enhanced by stronger backbones and a longer training duration. The “DCNv2” refers to deformable convolution v2 [91].

**Global kernel bank.** Table 2(c) presents the ablation study on the choice of the mask head paths used in the training stage. The first row is dynamic-kernel baseline that obtains 28.3  $AP_e^m$ , using only the dynamic kernel weights for all layers. Simply using static weights in the last one or two layers improves the  $AP_e^m$  by 0.6 and 0.8, as shown in the second and third rows. The best performance is achieved from including all the seven paths ( $\theta_1, \theta_2, \dots, \theta_7$ ). This allows the model to achieve the right balance between becoming aware of the common properties of entities (*e.g.*, textures or edges) and preserving a decent entity discriminability.

**High-performance regime.** Table 2(d) shows the performance of our proposed method in the high-performance training regime: stronger backbones and a longer training duration. With the longer training duration, we carry out training with a batch size of 16 for 36 epochs. We decay the learning rate with 0.1 factor at the 33-th and 35-th epochs. The models trained with our method benefit from the various techniques of high-performance training regime. The strongest one with ResNet-101 and Deformable Convolution v2 [91] obtains 35.5  $AP_e^m$ , and thus it is used for the cross-dataset visualization in the next section.

**Comparison with panoptic segmentation methods.** In Table 3, we compare our segmentation method with PanopticFPN [33], and DETR [7], PanopticFCN [39], and MaskFormer [11]. As shown in the second and third column, the numbers of  $AP_e^m$  are also smaller than PQ’s under the similar class-specific training models. This is because PQ merely uses a single IoU threshold of 0.5 to determine true positives, while our stricter  $AP_e^m$  considers a range of IoU thresholds ranging from 0.5 to 0.95 with a step size of 0.05. In the last two columns, the models with class-agnostic training consistently perform better in  $AP_e^m$  than the class-specific ones. This observation reaffirms the importance of our entity segmentation task that prioritizes mask quality over semantic classification. Our

Model	(S-S) PQ	(S-A) $AP_e^m$	(A-A) $AP_e^m$
PanopticFPN [33]	41.5	25.2	-
PanopticFCN [39]	43.6	26.5	28.5
PanopticDETR [7]	43.4	26.8	29.2
MaskFormer [11]	46.5	29.4	31.2
Ours	-	-	<b>31.8</b>

Table 3. **Comparison with panoptic segmentation methods.** The different train-test settings are: (S-S) class-specific training & class-specific testing; (S-A) class-specific training & class-agnostic testing; (A-A) class-agnostic training & class-agnostic testing. The PQ and  $AP_e^m$  are the evaluation metrics of panoptic segmentation and ES. Note that all models here are trained until full convergence by using long training schedules<sup>1</sup>.

model obtains the best performance by virtue of our two elaborately-designed modules that effectively exploit the unique class-agnostic and non-overlapping requirements of the task. Moreover, owing to the unified center-based representation and convolutional architecture, our method merely requires 36 training epochs to train the model to full convergence, compared to the hefty 300 epochs needed by Transformer-based methods [7, 11]. Thus, our method is significantly more accessible to many of the researchers and practitioners who have limited compute resources.

## 6.2. Cross-Dataset Evaluation

To demonstrate the generalization advantage of our entity segmentation task, we consider the setting where the evaluation set comes from a dataset different than the one/ones used for training. Here, we experiment with COCO and ADE20K. All these two datasets are converted into the ES format. For fair comparisons, all models are trained with pre-sampled 138,497 images (118,287 from COCO and 20,210 from ADE20K) regardless which datasets are used. PanopticFCN and DETR are trained for 12 and 300 epochs respectively, following their

<sup>1</sup>The convolution-based (PanopticFPN, PanopticFCN and ours) and the transformer-based frameworks (DETR and MaskFormer) adopt 36 and 300 training epochs, respectively. They all share the same ResNet50 backbone.

Dataset	COCO	ADE20K	CO+A	Dataset	COCO	Transformer	COCO	ADE20K
COCO	24.5/26.5/ <b>29.8</b>	15.4/16.6/ <b>19.4</b>	25.8/27.8/ <b>30.6</b>	COCO	24.8/29.2/ <b>31.8</b>	Swin-T [47]	35.0	33.2
ADE20K	15.2/17.5/ <b>20.1</b>	20.6/21.3/ <b>24.1</b>	23.8/24.9/ <b>26.3</b>	ADE20K	16.4/18.9/ <b>21.1</b>	Swin-L [47]	<b>38.9</b>	<b>37.0</b>
CO+A	22.1/23.8/ <b>27.0</b>	16.6/17.8/ <b>20.5</b>	24.9/26.6/ <b>28.9</b>	CO+A	22.9/26.3/ <b>28.7</b>	MiT-B5 [79]	37.4	35.6
(a)				(b)		(c)		

Table 4. Cross-dataset evaluation via the comparisons with (a) **PanopticFCN** [39] and (b) **DETR** [7]. Each column and row represent the training and validation dataset we use, respectively. "CO+A" means we use both COCO and ADE20K training datasets. Each cell element in Table (a)/(b) corresponds to the results of: (1) PanopticFCN/DETR with class-specific training; (2) with class-agnostic training; (3) Ours with 12 epochs in (a) and 36 epochs in (b). (c): The results of using stronger backbones to train on the merged COCO+ADE20K dataset.

original implementations. Our models with Transformer backbones [47, 79] are trained for 36 epochs. Please refer to the supplementary file for details.

**Quantitative evaluation.** Table 4(a) and (b) shows the performance comparisons with PanopticFCN [39] and DETR [7] in the cross-dataset setting. From those two tables, it can be clearly seen that our models generalizes better in the cross-dataset setting. In Table 4(a), the model trained on only COCO dataset obtains 29.8 and 20.1  $AP_c^m$  on COCO and ADE20K validation sets, signifying the superior generalization advantages of our task and proposed segmentation framework.

However, the COCO-trained model performs worse on ADE20K (29.8 $\rightarrow$ 20.1  $AP_c^m$ ). There are two reasons: (1) certain classes common to COCO and ADE20K are distinguished as *thing* and *stuff* differently; (2) ADE20K has more noisy annotations. Thus it may unreasonably penalize the good mask predictions from our model, which conflict with the annotations of other datasets due to large annotation gaps. Despite that, the qualitative results of ADE20K that we include in the supplementary file indicate that our model achieves a reasonably good performance. Also, there is a big performance gap on COCO validation step between using COCO and ADE20K for training. This is caused by ADE20K's low number (20,210) of training samples that are insufficient to train the model well.

One interesting aspect of our proposed task and framework is that multiple datasets of different domains can be directly combined to form a large training dataset. This advantage still remains when the models are trained to full convergence, as shown in Table 4(b). The aforementioned COCO $\rightarrow$ ADE20K problem is easily solved by combining COCO and ADE20K (COCO+A) for training without resolving label conflicts. In that case, the model achieves the best overall performance on all datasets. Furthermore, Table 4(c) shows that using strong Transformer backbones can further bridge the performance gaps between the two.

**Qualitative results.** Fig. 4 shows the our model's qualitative results on ImageNet. The model used here is based on the R-101-DCNV2 backbone described in Table 2(d) and trained only on COCO dataset. Some rare entities are accurately segmented even though they



Figure 4. The illustration of our model's generalization ability. We train the model in COCO dataset but apply it to ImageNet images. Note that most segmented entities are outside of COCO classes, never appear in the training set. Please refer to the supplementary file for many more cross-dataset qualitative results on ADE20K [90], Cityscapes [12], Places2 [89], and Objects365 [63].

## 7. Conclusion

This paper proposes a new task named entity segmentation (ES) which is aimed to serve downstream applications such as image manipulation/editing that have high requirements for segmentation mask quality but not for class labels. In this regard, an entity is defined as any semantically-meaningful and -coherent segment in the image. In the absence of semantic labels, we design a new metric  $AP_c$  to measure the ES performance. To effectively represent entities, we introduce a segmentation framework based on the unified center-based representation to handle both *thing* and *stuff* in this task. The proposed global kernel bank and overlap suppression modules further improve the segmentation performance. Experiments show that the models trained for ES task demonstrate strong generalization strengths and they perform exceptionally well in the open-world (cross-dataset) setting.

**Limitation.** Although the cross-dataset quantitative evaluation can assess the model's generalization performance, it is not impeccable. It may unreasonably penalize the good mask predictions from our model, which conflict with the annotations of other datasets due to large annotation gaps. This conflict would be well resolved if we built a new validation dataset spanning various domains but with consistent annotations, which we leave for future work.



## References

- [1] Bogdan Alexe, Thomas Deselaers, and Vittorio Ferrari. What is an object? In *CVPR*, 2010. 3
- [2] Connelly Barnes, Eli Shechtman, Adam Finkelstein, and Dan B Goldman. Patchmatch: A randomized correspondence algorithm for structural image editing. *TOG*, 2009. 1
- [3] Abhijit Bendale and Terrance Boulton. Towards open world recognition. In *CVPR*, 2015. 3
- [4] Ali Borji, Ming-Ming Cheng, Qibin Hou, Huaizu Jiang, and Jia Li. Salient object detection: A survey. *Computational visual media*, 2019. 2
- [5] Ali Borji, Ming-Ming Cheng, Huaizu Jiang, and Jia Li. Salient object detection: A benchmark. *TIP*, 2015. 2
- [6] Kaidi Cao, Yu Rong, Cheng Li, Xiaoou Tang, and Chen Change Loy. Pose-robust face recognition via deep residual equivariant mapping. In *CVPR*, 2018. 1
- [7] Nicolas Carion, Francisco Massa, Gabriel Synnaeve, Nicolas Usunier, Alexander Kirillov, and Sergey Zagoruyko. End-to-end object detection with transformers. In *ECCV*, 2020. 1, 2, 3, 7, 8
- [8] Liang-Chieh Chen, George Papandreou, Florian Schroff, and Hartwig Adam. Rethinking atrous convolution for semantic image segmentation. *arXiv:1706.05587*, 2017. 1, 2
- [9] Liang-Chieh Chen, Yukun Zhu, George Papandreou, Florian Schroff, and Hartwig Adam. Encoder-decoder with atrous separable convolution for semantic image segmentation. In *ECCV*, 2018. 1, 2
- [10] Xiaokang Chen, Kwan-Yee Lin, Jingbo Wang, Wayne Wu, Chen Qian, Hongsheng Li, and Gang Zeng. Bi-directional cross-modality feature propagation with separation-and-aggregation gate for rgb-d semantic segmentation. In *ECCV*, 2020. 2
- [11] Bowen Cheng, Alexander G Schwing, and Alexander Kirillov. Per-pixel classification is not all you need for semantic segmentation. In *NeurIPS*, 2021. 2, 7
- [12] Marius Cordts, Mohamed Omran, Sebastian Ramos, Timo Rehfeld, Markus Enzweiler, Rodrigo Benenson, Uwe Franke, Stefan Roth, and Bernt Schiele. The cityscapes dataset for semantic urban scene understanding. In *CVPR*, 2016. 1, 8
- [13] Jifeng Dai, Kaiming He, and Jian Sun. Instance-aware semantic segmentation via multi-task network cascades. In *CVPR*, 2016. 1, 2, 4
- [14] Jifeng Dai, Yi Li, Kaiming He, and Jian Sun. R-FCN: object detection via region-based fully convolutional networks. In *NeurIPS*, 2016. 3
- [15] Jifeng Dai, Haozhi Qi, Yuwen Xiong, Yi Li, Guodong Zhang, Han Hu, and Yichen Wei. Deformable convolutional networks. In *ICCV*, 2017. 1
- [16] Soheil Darabi, Eli Shechtman, Connelly Barnes, Dan B Goldman, and Pradeep Sen. Image melding: Combining inconsistent images using patch-based synthesis. *TOG*, 2012. 1
- [17] Infant Cognition Laboratory (UC Davis). Infant Categorization Development. <https://oakeslab.ucdavis.edu/infant-categorization-development.html>. 1
- [18] A. R. Dhamija, M. Günther, J. Ventura, and T. E. Boulton. The overlooked elephant of object detection: Open set. In *WACV*, 2020. 3
- [19] Piotr Dollár and C Lawrence Zitnick. Fast edge detection using structured forests. In *PAMI*, 2015. 3
- [20] Ross Girshick, Jeff Donahue, Trevor Darrell, and Jitendra Malik. Rich feature hierarchies for accurate object detection and semantic segmentation. In *CVPR*, 2014. 3
- [21] Kaiming He, Georgia Gkioxari, Piotr Dollár, and Ross Girshick. Mask r-cnn. In *ICCV*, 2017. 1, 2, 4
- [22] Kaiming He, Xiangyu Zhang, Shaoqing Ren, and Jian Sun. Deep residual learning for image recognition. In *CVPR*, 2016. 1, 6
- [23] Jie Hu, Li Shen, and Gang Sun. Squeeze-and-excitation networks. In *CVPR*, 2018. 1
- [24] R. Hu, P. Dollár, K. He, T. Darrell, and R. Girshick. Learning to segment every thing. In *CVPR*, 2018. 3
- [25] Gao Huang, Zhuang Liu, Laurens Van Der Maaten, and Kilian Q Weinberger. Densely connected convolutional networks. In *CVPR*, 2017. 1
- [26] Zilong Huang, Xinggang Wang, Lichao Huang, Chang Huang, Yunchao Wei, and Wenyu Liu. Ccnet: Criss-cross attention for semantic segmentation. In *ICCV*, 2019. 1, 2
- [27] Phillip Isola, Jun-Yan Zhu, Tinghui Zhou, and Alexei A Efros. Image-to-image translation with conditional adversarial networks. In *CVPR*, 2017. 1
- [28] Ayush Jaiswal, Yue Wu, Pradeep Natarajan, and Premkumar Natarajan. Class-agnostic object detection. In *WACV*, 2021. 1
- [29] Ayush Jaiswal, Yue Wu, Pradeep Natarajan, and Premkumar Natarajan. Class-agnostic object detection. In *WACV*, 2021. 3
- [30] Xu Jia, Bert De Brabandere, Tinne Tuytelaars, and Luc Van Gool. Dynamic filter networks. In *NeurIPS*, 2016. 5
- [31] Huaizu Jiang, Jingdong Wang, Zejian Yuan, Yang Wu, Nanning Zheng, and Shipeng Li. Salient object detection: A discriminative regional feature integration approach. In *CVPR*, 2013. 2
- [32] K J Joseph, Salman Khan, Fahad Shahbaz Khan, and Vineeth N Balasubramanian. Towards open world object detection. In *CVPR*, 2021. 3
- [33] Alexander Kirillov, Ross Girshick, Kaiming He, and Piotr Dollár. Panoptic feature pyramid networks. In *CVPR*, 2019. 1, 2, 4, 6, 7
- [34] Alexander Kirillov, Kaiming He, Ross Girshick, Carsten Rother, and Piotr Dollár. Panoptic segmentation. In *CVPR*, 2019. 1, 2
- [35] Alex Krizhevsky, Ilya Sutskever, and Geoffrey E Hinton. Imagenet classification with deep convolutional neural networks. In *NeurIPS*, 2012. 1
- [36] Anat Levin, Dani Lischinski, and Yair Weiss. Colorization using optimization. *ACM SIGGRAPH*, 2004. 1
- [37] Guanbin Li and Yizhou Yu. Deep contrast learning for salient object detection. In *CVPR*, 2016. 2

- [38] Yi Li, Haozhi Qi, Jifeng Dai, Xiangyang Ji, and Yichen Wei. Fully convolutional instance-aware semantic segmentation. In *CVPR*, 2017. 1, 2, 4
- [39] Yanwei Li, Hengshuang Zhao, Xiaojuan Qi, Liwei Wang, Zeming Li, Jian Sun, and Jiaya Jia. Fully convolutional networks for panoptic segmentation. In *CVPR*, 2021. 1, 2, 4, 5, 6, 7, 8
- [40] Tsung-Yi Lin, Piotr Dollár, Ross Girshick, Kaiming He, Bharath Hariharan, and Serge Belongie. Feature pyramid networks for object detection. In *CVPR*, 2017. 3, 5
- [41] Tsung-Yi Lin, Priya Goyal, Ross Girshick, Kaiming He, and Piotr Dollár. Focal loss for dense object detection. In *ICCV*, 2017. 2, 3, 4
- [42] Tsung-Yi Lin, Michael Maire, Serge Belongie, James Hays, Pietro Perona, Deva Ramanan, Piotr Dollár, and C Lawrence Zitnick. Microsoft coco: Common objects in context. In *ECCV*, 2014. 1, 2, 6
- [43] Chenxi Liu, Liang-Chieh Chen, Florian Schroff, Hartwig Adam, Wei Hua, Alan L Yuille, and Li Fei-Fei. Auto-deeplab: Hierarchical neural architecture search for semantic image segmentation. In *CVPR*, 2019. 1, 2
- [44] Huanyu Liu, Chao Peng, Changqian Yu, Jingbo Wang, Xu Liu, Gang Yu, and Wei Jiang. An end-to-end network for panoptic segmentation. In *CVPR*, 2019. 2
- [45] Rosanne Liu, Joel Lehman, Piero Molino, Felipe Petroski Such, Eric Frank, Alex Sergeev, and Jason Yosinski. An intriguing failing of convolutional neural networks and the coordconv solution. In *NeurIPS*, 2018. 5
- [46] Shu Liu, Lu Qi, Haifang Qin, Jianping Shi, and Jiaya Jia. Path aggregation network for instance segmentation. In *CVPR*, 2018. 1, 2, 4
- [47] Ze Liu, Yutong Lin, Yue Cao, Han Hu, Yixuan Wei, Zheng Zhang, Stephen Lin, and Baining Guo. Swin transformer: Hierarchical vision transformer using shifted windows. In *ICCV*, 2021. 8
- [48] Ziwei Liu, Zhongqi Miao, Xiaohang Zhan, Jiayun Wang, Boqing Gong, and Stella X Yu. Large-scale long-tailed recognition in an open world. In *CVPR*, 2019. 3
- [49] Jonathan Long, Evan Shelhamer, and Trevor Darrell. Fully convolutional networks for semantic segmentation. In *CVPR*, 2015. 1, 2
- [50] F Milletari, N Navab, SAV Ahmadi, and V-net. Fully convolutional neural networks for volumetric medical image segmentation. In *3DV*, 2016. 5
- [51] Douglas Morrison, Adam W Tow, M McTaggart, R Smith, N Kelly-Boxall, S Wade-McCue, J Erskine, R Grinover, A Gurman, T Hunn, et al. Cartman: The low-cost cartesian manipulator that won the amazon robotics challenge. In *ICRA*, 2018. 1
- [52] Patrick Pérez, Michel Gangnet, and Andrew Blake. Poisson image editing. *ACM SIGGRAPH*, 2003. 1
- [53] Pedro O. Pinheiro, Ronan Collobert, and Piotr Dollár. Learning to segment object candidates. In *NeurIPS*, 2015. 3
- [54] Lu Qi, Li Jiang, Shu Liu, Xiaoyong Shen, and Jiaya Jia. Amodal instance segmentation with kins dataset. In *CVPR*, 2019. 1
- [55] Lu Qi, Jason Kuen, Jiuxiang Gu, Zhe Lin, Yi Wang, Yukang Chen, Yanwei Li, and Jiaya Jia. Multi-scale aligned distillation for low-resolution detection. In *CVPR*, 2021. 3
- [56] Lu Qi, Shu Liu, Jianping Shi, and Jiaya Jia. Sequential context encoding for duplicate removal. In *Advances in Neural Information Processing Systems*, 2018. 4
- [57] Lu Qi, Yi Wang, Yukang Chen, Yingcong Chen, Xiangyu Zhang, Jian Sun, and Jiaya Jia. Pointins: Point-based instance segmentation. *TPAMI*, 2021. 1, 2, 4, 5
- [58] Xuebin Qin, Zichen Zhang, Chenyang Huang, Chao Gao, Masood Dehghan, and Martin Jagersand. Basnet: Boundary-aware salient object detection. In *CVPR*, 2019. 2
- [59] Shafin Rahman, Salman Khan, and Fatih Porikli. Zero-shot object detection: Learning to simultaneously recognize and localize novel concepts. In *ACCV*, 2018. 1
- [60] Shaoqing Ren, Kaiming He, Ross B. Girshick, and Jian Sun. Faster R-CNN: towards real-time object detection with region proposal networks. In *NeurIPS*, 2015. 1, 3
- [61] Yu Rong, Ziwei Liu, Cheng Li, Kaidi Cao, and Chen Change Loy. Delving deep into hybrid annotations for 3d human recovery in the wild. In *ICCV*, 2019. 1
- [62] Yu Rong, Takaaki Shiratori, and Hanbyul Joo. Frankmocap: Fast monocular 3d hand and body motion capture by regression and integration. *arXiv preprint arXiv:2008.08324*, 2020. 1
- [63] Shuai Shao, Zeming Li, Tianyuan Zhang, Chao Peng, Gang Yu, Xiangyu Zhang, Jing Li, and Jian Sun. Objects365: A large-scale, high-quality dataset for object detection. In *Proceedings of the IEEE/CVF International Conference on Computer Vision*, pages 8430–8439, 2019. 8
- [64] Guang Shu. Human detection, tracking and segmentation in surveillance video. 2014. 1
- [65] Karen Simonyan and Andrew Zisserman. Very deep convolutional networks for large-scale image recognition. In *ICLR*, 2015. 1
- [66] Jian Sun, Lu Yuan, Jiaya Jia, and Heung-Yeung Shum. Image completion with structure propagation. *TOG*, 2005. 1
- [67] Christian Szegedy, Sergey Ioffe, Vincent Vanhoucke, and Alex Alemi. Inception-v4, inception-resnet and the impact of residual connections on learning. In *arXiv*, 2016. 1
- [68] Christian Szegedy, Vincent Vanhoucke, Sergey Ioffe, Jon Shlens, and Zbigniew Wojna. Rethinking the inception architecture for computer vision. In *CVPR*, 2016. 1
- [69] Richard Szeliski. *Computer vision: algorithms and applications*. Springer Science & Business Media, 2010. 2
- [70] Zhi Tian, Chunhua Shen, and Hao Chen. Conditional convolutions for instance segmentation. In *ECCV*, 2020. 1, 2, 4, 5, 6
- [71] Zhi Tian, Chunhua Shen, Hao Chen, and Tong He. Fcos: Fully convolutional one-stage object detection. In *ICCV*, 2019. 2, 3, 4, 5
- [72] Inam Ullah, Muwei Jian, Sumaira Hussain, Jie Guo, Hui Yu, Xing Wang, and Yilong Yin. A brief survey of visual saliency detection. *Multimedia Tools and Applications*, 2020. 2
- [73] Ting-Chun Wang, Ming-Yu Liu, Jun-Yan Zhu, Andrew Tao, Jan Kautz, and Bryan Catanzaro. High-resolution image synthesis and semantic manipulation with conditional gans. *arXiv:1711.11585*, 2017. 1

- [74] Weiyao Wang, Matt Feiszli, Heng Wang, and Du Tran. Unidentified video objects: A benchmark for dense, open-world segmentation. *arXiv preprint arXiv:2104.04691*, 2021. 3
- [75] Xinlong Wang, Tao Kong, Chunhua Shen, Yuning Jiang, and Lei Li. Solo: Segmenting objects by locations. In *ECCV*, 2020. 1, 2, 4
- [76] Xinlong Wang, Rufeng Zhang, Tao Kong, Lei Li, and Chunhua Shen. Solov2: Dynamic and fast instance segmentation. In *NeurIPS*, 2020. 1, 2, 4, 5
- [77] Yi Wang, Xin Tao, Xiaojuan Qi, Xiaoyong Shen, and Jiaya Jia. Image inpainting via generative multi-column convolutional neural networks. In *NeurIPS*, 2018. 1
- [78] Enze Xie, Peize Sun, Xiaoge Song, Wenhai Wang, Xuebo Liu, Ding Liang, Chunhua Shen, and Ping Luo. Polarmask: Single shot instance segmentation with polar representation. In *CVPR*, 2020. 1, 2, 4
- [79] Enze Xie, Wenhai Wang, Zhiding Yu, Anima Anandkumar, Jose M Alvarez, and Ping Luo. Segformer: Simple and efficient design for semantic segmentation with transformers. In *NeurIPS*, 2022. 3, 8
- [80] Yajie Xing, Jingbo Wang, and Gang Zeng. Malleable 2.5 d convolution: Learning receptive fields along the depth-axis for rgb-d scene parsing. In *ECCV*, 2020. 2
- [81] Yuwen Xiong, Renjie Liao, Hengshuang Zhao, Rui Hu, Min Bai, Ersin Yumer, and Raquel Urtasun. Upsnet: A unified panoptic segmentation network. In *CVPR*, 2019. 1, 2, 4
- [82] Changqian Yu, Jingbo Wang, Changxin Gao, Gang Yu, Chunhua Shen, and Nong Sang. Context prior for scene segmentation. In *CVPR*, 2020. 2
- [83] Changqian Yu, Jingbo Wang, Chao Peng, Changxin Gao, Gang Yu, and Nong Sang. Bisenet: Bilateral segmentation network for real-time semantic segmentation. In *ECCV*, 2018. 2
- [84] Changqian Yu, Jingbo Wang, Chao Peng, Changxin Gao, Gang Yu, and Nong Sang. Learning a discriminative feature network for semantic segmentation. In *CVPR*, 2018. 2
- [85] Jiahui Yu, Zhe Lin, Jimei Yang, Xiaohui Shen, Xin Lu, and Thomas S Huang. Generative image inpainting with contextual attention. In *CVPR*, 2018. 1
- [86] Jiahui Yu, Zhe Lin, Jimei Yang, Xiaohui Shen, Xin Lu, and Thomas S Huang. Free-form image inpainting with gated convolution. In *ICCV*, 2019. 1
- [87] Hengshuang Zhao, Jianping Shi, Xiaojuan Qi, Xiaogang Wang, and Jiaya Jia. Pyramid scene parsing network. In *CVPR*, 2017. 1, 2
- [88] Hengshuang Zhao, Yi Zhang, Shu Liu, Jianping Shi, Chen Change Loy, Dahua Lin, and Jiaya Jia. Pscanet: Point-wise spatial attention network for scene parsing. In *ECCV*, 2018. 1, 2
- [89] Bolei Zhou, Agata Lapedriza, Aditya Khosla, Aude Oliva, and Antonio Torralba. Places: A 10 million image database for scene recognition. *IEEE transactions on pattern analysis and machine intelligence*, 40(6):1452–1464, 2017. 8
- [90] Bolei Zhou, Hang Zhao, Xavier Puig, Sanja Fidler, Adela Barriuso, and Antonio Torralba. Scene parsing through ade20k dataset. In *CVPR*, 2017. 1, 2, 8
- [91] Xizhou Zhu, Han Hu, Stephen Lin, and Jifeng Dai. Deformable convnets v2: More deformable, better results. In *CVPR*, 2019. 1, 7